

Ocean-surface and wind dynamics in the Atlantic Ocean off Northwest Africa during the last 140 000 years

J.-A. Flores *, M.A. Bárcena, F.J. Sierro

Departamento de Geología, Universidad de Salamanca, 37008 Salamanca, Spain

Received 19 March 1999; accepted for publication 14 March 2000

Abstract

A combined micropaleontological analysis of core CAMEL-1, from the oligotrophic Sierra Leone Rise area, has allowed reconstruction of the paleoclimatic and paleoceanographic history of the region for the last 140 kyr. The ratio (N) between the Reticulofenestrads (coccolithophore indicators of relatively high nutrient contents) versus *Florisphaera profunda* (a Lower Photoc Zone coccolithophore) allowed us to monitor changes in the nutricline depth. These results were compared with those obtained for marine diatom and planktic foraminifera assemblages. Thus, a shallow nutricline/thermocline (and high productivity) during stages 6, 5d, 5b, 4 and 2 is proposed. This situation can be correlated with maximum input of biosiliceous wind-transported particles (fresh-water diatoms and phytoliths) in sea sediments. The shallow nutricline is correlated with an intensification in Atlantic divergence and/or a North Equatorial Current intensification, when the NE trades were enhanced for glacial and stadials (cold) periods. A clear precessional component is observed in the surface water dynamics during the last climatic cycle, minima in the N ratio coinciding with minimum insolation during winter in the Boreal hemisphere. During MIS 5, 4 and 2 dry conditions were dominant on the northern African continent, corresponding to a more intense NE trade wind circulation. The increased phytolith concentrations during MIS 6 are consistent with a more intense seasonality on the African continent. Cold planktic foraminifera assemblages show an eccentricity component linked to northern Ice-sheet dynamics. This situation is enhanced in isotope stages 6 and 3, due to an intensification in the North Equatorial Current. The eccentricity component is also observed both in the N ratio (coccolithophore-related) and in the total planktic foraminifera. © 2000 Elsevier Science B.V. All rights reserved.

Keywords: Atlantic Ocean; coccolithophores; diatoms; paleoceanography; paleoproductivity; planktic foraminifera; Pleistocene; phytoliths; West Africa

1. Introduction

Surficial water dynamics are mainly controlled by wind systems. Differences in wind intensity and direction also control nutrient contents and ocean primary production, affecting the concentration of oceanic and atmospheric CO₂ reservoirs (Broecker,

1982). Analysis of autochthonous plankton organisms (coccolithophores, planktic foraminifera and marine diatoms) together with wind-transported microfossils from continental areas (fresh-water diatoms and phytoliths) offers the opportunity to link different signals with broad-scale regional events and to examine the temporal evolution of these microfossils.

Several authors have focused their studies on the eastern tropical Atlantic. Sarnthein et al.

* Corresponding author.

E-mail address: flores@gugu.usal.es (J.-A. Flores)

(1982) and Ruddiman et al. (1989) summarized climatic evolution through the Neogene, using micropaleontological, biogeochemical and sedimentological techniques. The CLIMAP project has also generated important data for the region as from the last glacial maximum (LGM). Other studies in the area have focused on coastal African upwelling and divergence regions, using micropaleontological, biogeochemical and sedimentological techniques are: Molfino and McIntyre (1990); Abrantes (1991); Lange et al. (1994); Jordan et al. (1996); Pokras and Mix (1985); Pokras (1987); Gasse et al. (1989); Jansen et al. (1989); Tiedemann et al. (1989); Ruddiman and Janecek (1989); Jansen and Van Iperen (1991); Dupont et al. (1999), among others.

Several questions addressing the last 140 kyr in the oligotrophic eastern tropical Atlantic are proposed: (1) What were the surface water mass characteristics and the main oceanographic features like? (2) What relationship existed between nutricline/thermocline dynamics and wind regimes? (3) How did the calcareous nannofossil assemblages evolve in this context? (4) What relationship existed between the changes in surface water dynamics and continental climate?

2. Material and techniques

The CAMEL-1 gravity core was recovered during the CAMEL-93 BIO *Hespérides* (Spanish vessel) Cruise (CAñón Medioceánico Ecuatorial 1993) in the Sierra Leone Rise (Central Eastern Tropical Atlantic) at 5°6'25N/21°2'36W. Water depth at the core location is 2658 m. The total length of core CAMEL-1 is 446 cm, and the core consist of alternations of gray muddy sands, brown sandy muds and ochre sandy muds. An organic matter-rich level occurs at the top of CAMEL-1 (0–8 cm). Since our interest lay in the last 140 kyr, only the upper 160 cm segment of the core was examined. Samples were taken at the same core depths every 3 cm for calcareous nannoplankton, planktic foraminifera, and siliceous microfossils, as well as for sedimentological and isotopic analyses.

2.1. *Coccolithophores*

The slides used to inventory nannofossil assemblages were prepared using the methodology of Flores and Siervo (1997), which allows homogeneous and comparable data analysis between samples and the possibility of estimating total coccolith abundances. Coccolithophore analyses were made at 1250× magnification using a polarised-light microscope. For quantitative analysis, about 300 coccoliths >3 µm were counted per slide in a variable number of viewing fields. Nannofossils <3 µm were counted separately on the same fields of view analysed for large nannofossils. Thus, >1000 small coccoliths were counted. For less abundant species, additional viewing fields were analysed. Relative abundances of the selected species were used in order to trace dilution effects and to compare our data with those previously published.

Additionally, routine scanning electron microscope analyses were made in order to estimate the preservation state and morphological features in calcareous nannofossils.

For stratigraphic purposes, we plotted the relative abundance of counted coccoliths in order to follow a conventional pattern. For paleoecological and paleoceanographic studies, the number of coccoliths was converted to 'coccospheres' according to Knappertsbusch (1993) and Kleijne (1993) (see the Appendix).

Coccolithophore associations may reflect the nutrient content and the position in the water column. *Florisphaera profunda* is an inhabitant of the current tropical Lower Photic Zone (LPZ) in tropical and subtropical environments (Okada and Honjo, 1973). Molfino and McIntyre (1990, 1991) linked the abundance of *F. profunda* to changes in the nutricline/thermocline position. Besides, the abundance of Reticulofenestrads is generally interpreted as an indicator of upwelling intensity (or relatively high productivity) (Okada and Wells, 1997; Wells and Okada, 1996). To monitor nutricline (and thermocline) fluctuations, we propose the use of the *N* ratio between Reticulofenestrads (*R*) and *F. profunda* (*F*) abundances:

$$N = \frac{R}{R + F}$$

High values in the N ratio imply a relatively shallow nutricline/thermocline position. Low values are interpreted as a relatively deep nutricline/thermocline position.

2.2. Diatoms and phytoliths

Absolute diatom numbers were determined from microscope slides with randomly distributed microfossils. Cleaning of the sediment samples and preparation of permanent mounts for light microscopy were done according to the settling technique described by Abelmann et al. (2000). For counting routines, a light microscope at $1000\times$ magnification was used. In general, >400 fields of view were observed. Schrader and Gersonde's (1978) recommendations were used for diatom counting. The preservation status of the fossil assemblage was estimated by visual examination.

Additionally, the *PhFD* index (Jansen and Van Iperen, 1991) was calculated, according to the formula:

$$\text{PhFD} = \frac{\text{Ph}}{\text{Ph} + \text{FD}}$$

where Ph is the number of phytoliths and FD is the number of freshwater diatoms.

2.2.1. Planktic foraminifers and stable isotopes

After drying and weighing, samples were washed and sieved through 150 and 62 μm sieves, but only the $>150\ \mu\text{m}$ residues were used for counting. Residues were split to obtain a fraction of ca. 250 planktic foraminifera, which were identified and counted. Around 40 *Globigerinoides ruber* specimens of between 250 and 300 μm were picked and cleaned ultrasonically for oxygen isotope analysis. Organic matter was destroyed by heating up to 400°C under a vacuum over 2 h. The samples were then placed in a Sira-II (VG) spectrometer with orthophosphoric acid at 25°C . Results are expressed in PDB (Pee Dee Belemnite standard) in Table 1.

Micropaleontological slides and sieved samples are archived in the Micropaleontological Collections of the University of Salamanca.

Table 1
Core CAMEL-1 $\delta^{18}\text{O}$ data set, isotope analyses were obtained from *Globigerinoides ruber* specimens

cm	$\delta^{18}\text{O}_{\text{PDB}}$
0	-1.645
3	-1.663
7	-1.424
10	-1.379
13	-1.182
16	-0.706
19	-0.535
22	-0.501
25	-0.817
28	-0.674
32	-0.701
35	-0.771
38	-0.719
41	-0.729
44	-0.992
47	-0.927
53	-0.876
57	-0.940
60	-1.107
64	-1.391
70	-1.168
73	-1.617
76	-1.546
79	-1.502
82	-1.556
85	-1.547
88	-1.412
91	-1.297
94	-1.637
97	-1.688
100	-1.647
103	-1.504
107	-1.533
110	-1.567
113	-1.570
116	-1.659
120	-1.538
122	-1.800
125	-1.820
128	-1.696
131	-1.730
134	-1.625
137	-1.504
141	-0.762

3. Oceanographic settings

In today's Central Atlantic tropical and equatorial areas the major surface current system is

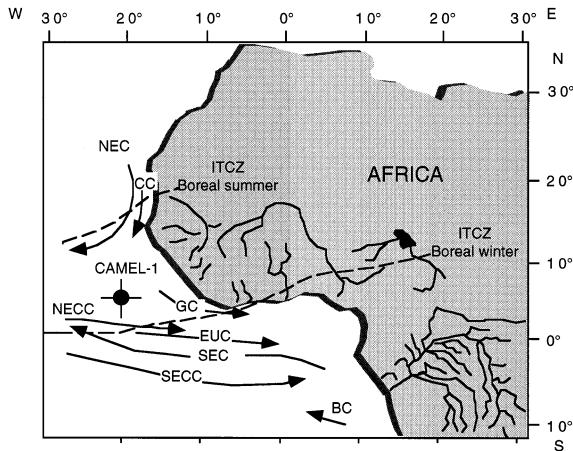


Fig. 1. Geographic location of core CAMEL-1, and atmospheric and oceanographic setting. Arrows represent current directions. NEC, North Equatorial Current; ITCZ, Intertropical Convergence Zone; NECC, North Equatorial Counter Current; GC, Guinea Current; CC, Canary Current; EUC, Equatorial Under Current; SEC, South Equatorial Current; and BC, Benguela Current.

characterized by two broad westward-flowing currents: the North Equatorial Current (NEC) and the South Equatorial Current (SEC) (Fig. 1). The comparatively narrow eastward-flowing North Equatorial Counter Current (NECC) separates these features. The NEC and SEC are a direct response to the NE and SE Trade winds. The boundary between the NE and SE trade winds is the Intertropical Convergence Zone (ITCZ), which fluctuates between 5 and 15°N in the east Atlantic (Höflich, 1984). Seasonal changes in the trade wind system control the surface-water dynamics in this area (Eriksen and Katz, 1987). During Northern Hemisphere summer the strong SE trades produce an increase in the SEC velocity, coinciding with the northernmost position of the ITCZ (Peterson and Stramma, 1991) (Fig. 1). In this setting, NECC shows its greatest eastwards advection (Garzoli and Katz, 1983; Richardson and Walsh, 1986), producing upwelling maxima, a shallow thermocline, and the lowest sea surface temperatures (SST) in the equatorial divergence area (Voituriez and Herland, 1977; Houghton, 1991). The eastward-flowing Equatorial Under Current (EUC), characterized by relatively high

temperatures and salinity (Verstraete, 1992), is weakly developed in this situation. During boreal winter the NE trades become stronger and the ITCZ reaches its southerly position, resulting in an enhanced NEC and Guinea Current (GC) (southern branch of the Canary Current, CC). Advection of the SEC and NECC decreases while warm saline water is introduced eastward by the EUC (Katz et al., 1981). During the boreal winter, a typical tropical situation is characterized by higher SST, a lower nutrient content a deep chlorophyll maximum (Voituriez and Herland, 1977), and a deep thermocline (Houghton, 1991). The NE Trades supply aeolian dust to the Atlantic Ocean (Schütz, 1980), which may enter the ITCZ and may thus influence oceanic sedimentation north of the equator (Treppke et al., 1996).

Within the above framework, core CAMEL-1 is situated in an oligo-mesotrophic area not directly linked to the equatorial and western African coastal upwellings. However, fluctuations in the divergence position and intensity may influence the surface-water characteristics in the area.

3.1. *Glacial–interglacial scenarios*

The African climate was clearly linked to that of high-latitude ice sheets and associated changes in sea-surface temperature in the high-latitude North Atlantic (Ruddiman et al., 1989), as well as variations in sea-surface temperature and evaporation in the tropical Atlantic and Africa continental climate (Rossignol-Strick, 1983; Tiedemann et al., 1989). The trade winds apparently became more vigorous during periods of ice growth and ceased shortly after the first major phase of polar deglaciation ca. 12 ka ago (Sarnthein et al., 1982; Stabell, 1986). The Harmattan Saharan Air Layer, a shallow trade wind layer, and the overlying easterly mid-tropospheric jet stream appear to drive the dust supply from Africa to the Atlantic Ocean (Prospero and Carlson, 1972; Kalu, 1979; Sarnthein et al., 1982). The dust flow is to the Easterly Waves (Tetzalaff and Wolter, 1980), a system of tropical disturbances connected to the ITCZ. During glacial times, tropical northwest Africa was driest during glaciations and stades, but wetter than at present during interglacials and

interstades (Pokras and Mix, 1987). The semi-desert vegetation in this region reached 15°N during glacials (Dupont, 1999). Conversely, central-equatorial Africa was most arid during interstades and times of ice growth, and more humid during deglaciations (Pokras and Mix, 1985), with a strong reduction in the rain forest and a reduction in the estimated run-off during glacials where, with some exceptions, savanna and dry open vegetation was dominant (Dupont and Hooghiemstra, 1989; Dupont and Agwu, 1992; Dupont and Weinelt, 1996; Ning and Dupont, 1997; Dupont, 1999; Dupont et al., 1999). At the same time, increases in coastal upwelling in north-west Africa (Abrantes, 1991) and in the east tropical-equatorial Africa area (Dupont et al., 1998) occurred during glacial periods. In the equa-

torial Atlantic, high abundances of wind-blown freshwater diatoms coincided with periods of ice growth and aridity, characterized by a lowering of lake levels and the exposure of soil rich in diatom remains (Stabell, 1986). The above-mentioned paleoclimatic reconstructions were based on data from oceanic sediments. Although according to Gardner and Hays (1976) the ITCZ did not migrate very far outside its present seasonal boundary during glacial times, other important features such as the intensity of upwelling systems or the intensity of some of the above mentioned currents underwent important modifications from glacial to interglacial conditions (Sarnthein et al., 1982). In the central equatorial Atlantic Ocean, the initial cooling of glacial periods was characterized by an intensification in equatorial upwelling intensifica-

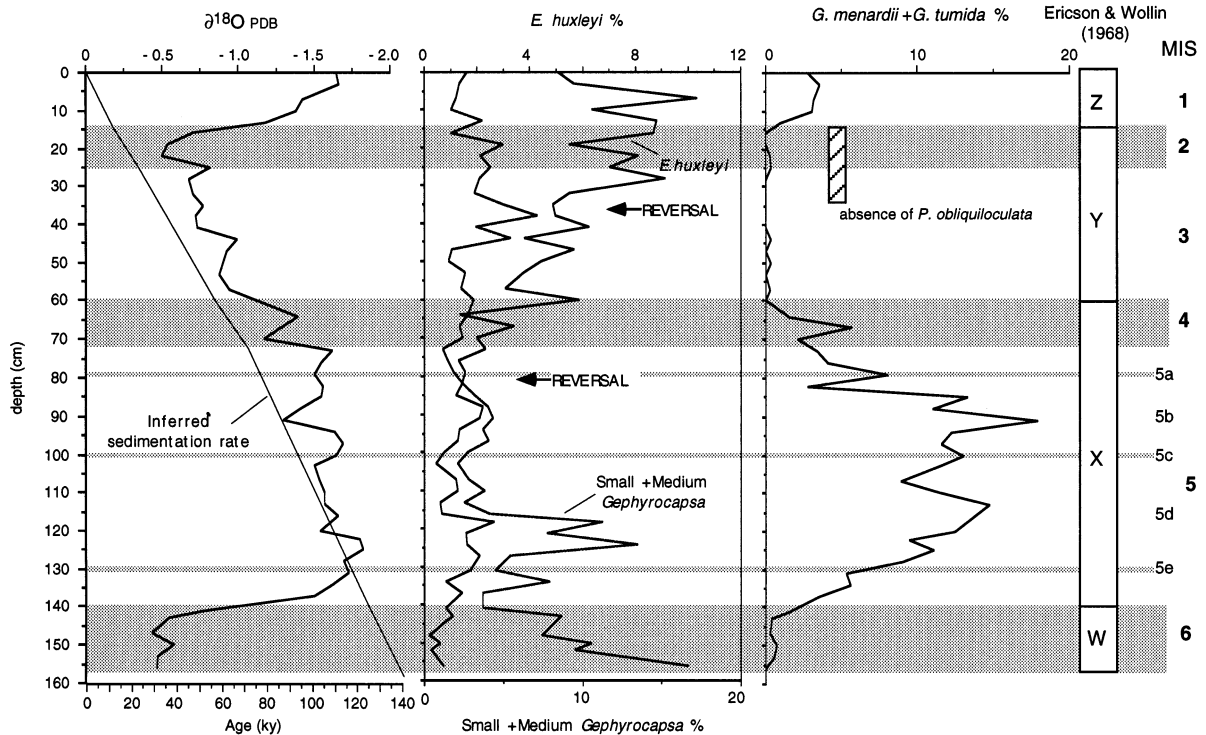


Fig. 2. Stable isotope ($\delta^{18}\text{O}$), coccolithophore and planktic foraminifera stratigraphies and estimated sedimentation rates for core CAMEL-1. Coccolithophore stratigraphy is based in the *Emiliania huxleyi* versus small plus medium sized *Gephyrocapsa* relative abundances. Planktic foraminifera zonations are based on Ericson and Wollin (1968). Ages are based on Martinson et al. (1987). For details see Section 4 in the text. MIS, marine isotope stages.

tion, followed by an intensified cooling, resulting from an increase in the Benguela Current advection (Mix and Morey, 1996; Jansen et al., 1996).

4. Stratigraphy

Core stratigraphy is mainly based on the oxygen isotope ($\delta^{18}\text{O}$) curve and some well-known biostratigraphic events (Fig. 2). The ages for the marine isotope stages (MIS) are based on Martinson et al. (1987). Interpretation of the $\delta^{18}\text{O}$ curve is based on the identification of several well-dated calcareous plankton events. Thierstein et al. (1977) observed a reversal in *Emiliana huxleyi*/*Gephyrocapsa caribbeanica* abundance at 80 kyr in middle latitudes. In core CAMEL-1 we observed a clear reversal considering the ‘medium *Gephyrocapsa*’ (between 3 and 5 μm) and the ‘small *Gephyrocapsa*’ (SG, <3 μm), together at the same stratigraphic level. We consider this event to be equivalent to that reported by Thierstein et al. (1977). Another reversal marked by a clear dominance in the abundance of *E. huxleyi* can also be observed at ca. 40 kyr. This latter event has also been observed by Jordan et al. (1996) and others. The first reversal is observed in MIS 5a, whereas the second one occurs during MIS 3 at this latitude (Fig. 2).

Planktic foraminiferal biostratigraphy is mainly based on the distribution of the *Globorotalia menardii* complex (*G. menardii* plus *Globorotalia tumida*) using the biostratigraphic zones (W, X, Y and Z) defined by Ericson and Wollin (1968). The Z zone, characterizing MIS 1, can be recognized in the uppermost 12 cm, while zone Y extends from 12 to 62 cm. The *G. menardii* complex is absent in this zone ranging from MIS 2 to 4. The boundary between MIS 4 and 5 is marked by the limit between zones Z and X, while the limit between zones X and W coincides with the MIS 5 and 6 transition (Fig. 2). *Pulleniatina obliquiloculata* is present from MIS 5 upwards with the exception of the middle part of zone Y, where it completely disappears. This interval extends from 13 to 35 cm in core CAMEL-1, ranging in age from 15 to 40 kyr (Bé et al., 1976) (Fig. 2).

These data allow us to suggest a continuous

sedimentation, with average sedimentation rates of ca. 1 cm kyr⁻¹.

5. Results

The coccolithophore assemblages mainly consist of *Florisphaera profunda*, and Reticulofenestrads (*Emiliana huxleyi* and ‘medium *Gephyrocapsa*’, principally *Gephyrocapsa muelleriae*, but occasionally small specimens of *Gephyrocapsa oceanica* and *Gephyrocapsa caribbeanica*, and ‘small *Gephyrocapsa*’ featuring *Gephyrocapsa ericsoni* and *Gephyrocapsa aperta*). Other species recorded in low proportions are plotted in Fig. 3. The most abundant biogenic siliceous particles are freshwater diatoms (*Aulacoseira granulata*, *Cyclotella ocellata* and *Cyclotella meneghiniana*) and phytoliths. Marine diatoms are recorded in minor proportions. Planktic foraminifera are the main component of the calcitic fraction of the sediment. The number of planktic foraminifera per gram of dry sediment is very variable showing high values during interglacial and low values during glacial stages. *Neogloboquadrina pachyderma* is the most abundant foraminiferal species. Further details about systematic features can be found in the Appendix.

Taking into account the above-mentioned stratigraphic pattern, several differential features are observed in the micropaleontological assemblages.

5.1. MIS 6

For this interval we recorded the highest abundances of coccolithophores (between 2 and 4×10^8 sphere equivalences g⁻¹), mainly due to the relative increase in SG and *Gephyrocapsa oceanica*, but these decrease dramatically after the MIS 6/5 boundary. The number of *Florisphaera profunda* spheres per gram is high during MIS 6, although this interval shows the lowest relative abundances, due to the high abundance of Reticulofenestrads (Figs. 3–5). Other taxa that show peaks during MIS 6 are *Umbilicosphaera* spp. (mainly *Umbilicosphaera sibogae* and minor proportions of *Umbilicosphaera hulburtiana*) and moderate proportions of *Syracosphaera* spp (Fig. 5).

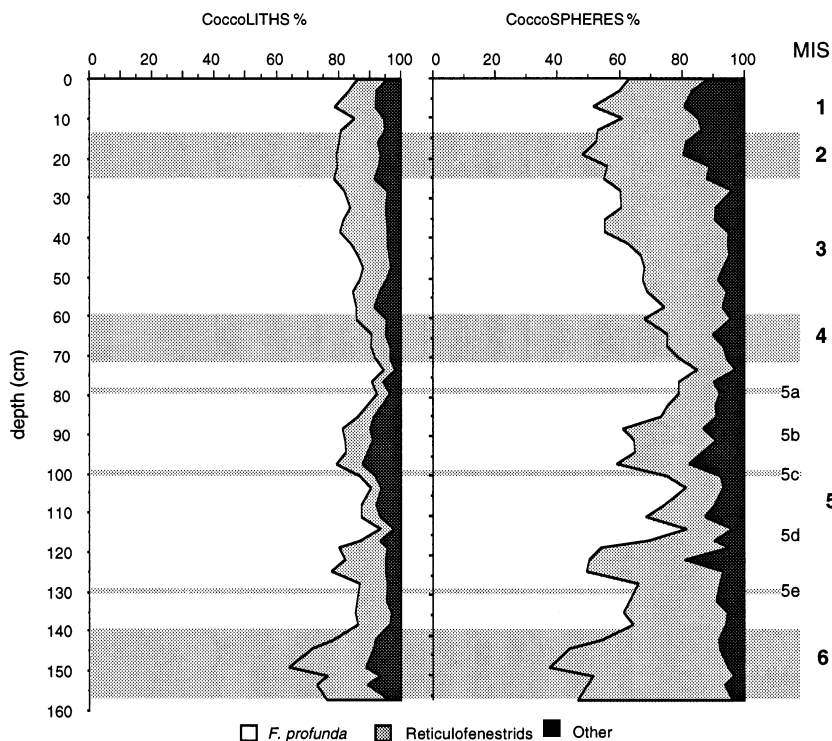


Fig. 3. Percentage abundances of the most significant Coccolithophores groups identified in core CAMEL-1, in coccoliths and coccospheres (see Appendix).

In MIS 6 phytoliths reach a significant peak, showing values of $2 \times 10^6 \text{ g}^{-1}$ of dry sediment. These values fall towards the MIS 6/5 boundary. In the same interval, *Aulacoseira granulata* occurs at low values ($< 1 \times 10^7$ valves per gram of sediment). High values in the PhFD index are observed (Fig. 6). The preservation of marine diatoms is moderate, showing relatively high values.

Foraminifers are in low abundance in MIS 6, reaching $< 1.75 \times 10^4$ shells g^{-1} of dry sediment. The foraminiferal assemblage in this interval is characterized by a strong increase in Neogloboquadrinids, especially the cold species *Neogloboquadrina pachyderma*, in which is the main species in the 'cold-transitional' assemblage (Fig. 7).

5.2. MIS 5

The total abundance of coccospheres in MIS 4 shows values ca. 1×10^8 coccosphere equivalences

per gram, with positive peaks at MIS 5e, 5a, and close to 5c (Fig. 5). The maximum abundance (both absolute and relative) in Reticulofenestrads occurs at the base of MIS 5d and 5b. In MIS 5e, the top of 5d, and 5a, we observed low values in the abundance of Reticulofenestrads. *Florisphaera profunda* and *Calcidiscus leptoporus* show peaks at MIS 5e, the base of 5c, and 5a. An important peak of *Syracosphaera* spp. (*Syracosphaera histrica* and *Syracosphaera pulchra*) coincides with MIS 5e and, in minor proportions, close to MIS 5c; a similar pattern is observed for *Helicosphaera* spp. *Umbilicosphaera* spp. show the lowest abundances in MIS 5e and close to the MIS 5/4 boundary, and an important peak in MIS 5c (Figs. 3–5).

In MIS 5, phytolith abundance is only ca. $0.5 \times 10^6 \text{ g}^{-1}$, which is the lowest value until the Holocene. Minimum values are recorded close to MIS 5e, 5c and 5a. In MIS 5 the fresh-water diatom *Aulacoseira granulata* occurs at a relatively

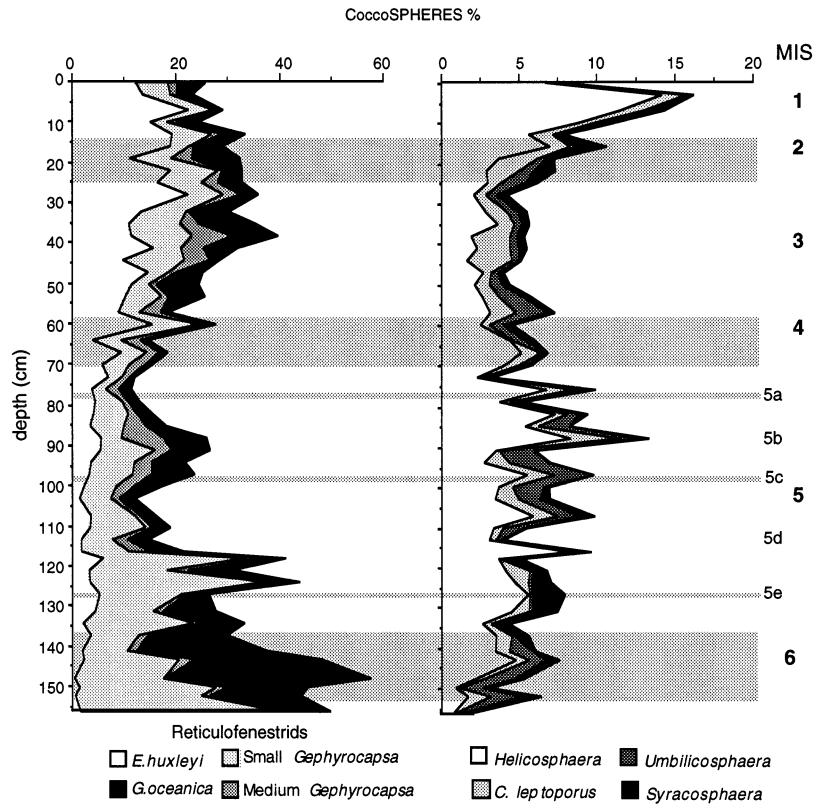


Fig. 4. Accumulated percentages of the most abundant coccolithophore species identified in core CAMEL-1.

high abundance. Peaks are observed close to the top of 5b and base of 5c, decreasing progressively along MIS 5a, where its abundance is $<10^6$ valves g^{-1} . Phytoliths and fresh-water diatoms do not follow a parallel pattern during this interval, with the exception of MIS 5d. In MIS 5 marine diatoms occur in low abundance in CAMEL-1. Upon observing the PhFD ratio, the lowest values in this stage occur from substage 5e to 5c, and high values during substage 5a (Fig. 6). Planktic foraminifera show higher values during interglacial substages and lower values during glacial substages (MIS 5b is especially significant). Subpolar and transitional species reach a prominent minimum during substage 5e, gradually increasing during substages 5d, 5c and 5a. However, MIS 5 is characterized by relatively low proportions of subpolar and transitional species (Fig. 7).

5.3. MIS 4

In MIS 4 the total abundance of coccospheres per gram has values of 1.5×10^8 . This interval is characterized by a progressive reduction in *Florisphaera profunda* from the MIS 5/4 boundary upwards. The Reticulofenestrads show the opposite trend, increasing progressively towards the top of MIS 4. *Umbilicosphaera* spp. and *Syracosphaera* spp. occur in low numbers, showing weak peaks. *Calcidiscus leptoporus* is recorded in low proportions during this interval. The number of phytoliths increases in MIS 4 and *Aulacoseira granulata* shows peak values ($>2.5 \times 10^6$ valves g^{-1}). Marine diatoms increase upwards from the MIS 5/4 boundary, reaching high values close to the MIS 4/3 boundary. The PhFD index shows in this period the lowest values (Fig. 6). In this interval, a promi-

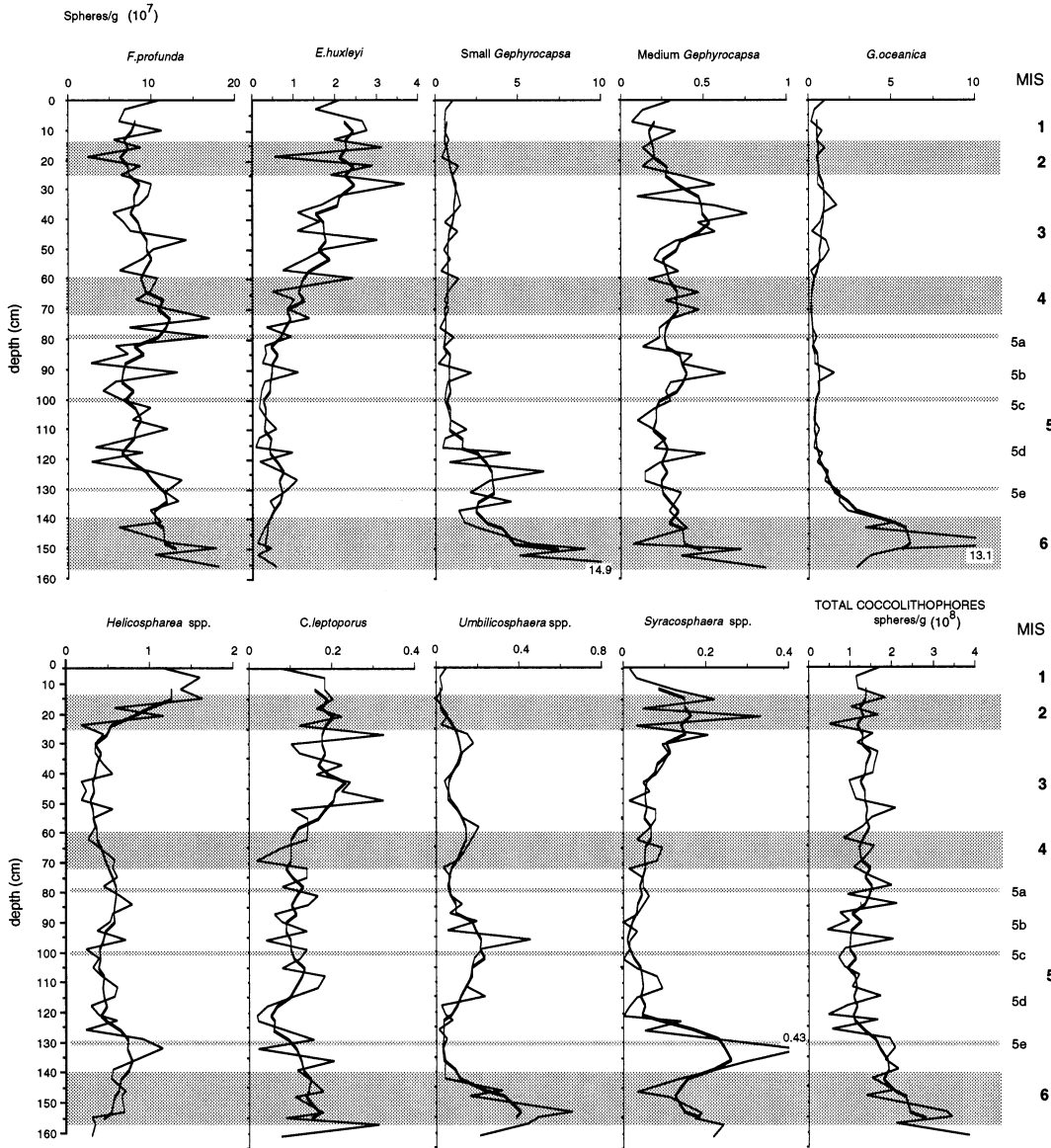


Fig. 5. Total abundance (coccosPHERES g^{-1}) of the most abundant coccolithophore species in core CAMEL-1. Thick lines are three point moving averages.

nent minima in foraminifera occur, while subpolar and subtropical forms increase upwards (Fig. 7).

5.4. MIS 3

In MIS 3 the total number of coccospheres per gram is similar to that observed for MIS 4.

MIS 3 exhibits a progressive increase in Reticulofenestrads and a reduction in *Florisphaera profunda*. *Calcidiscus leptopus* reaches maximum values in the middle part of MIS 3, whereas *Umbilicosphaera* spp. and *Syracosphaera* spp. occur in low numbers in the same interval, although their abundance increases towards the MIS 3/2

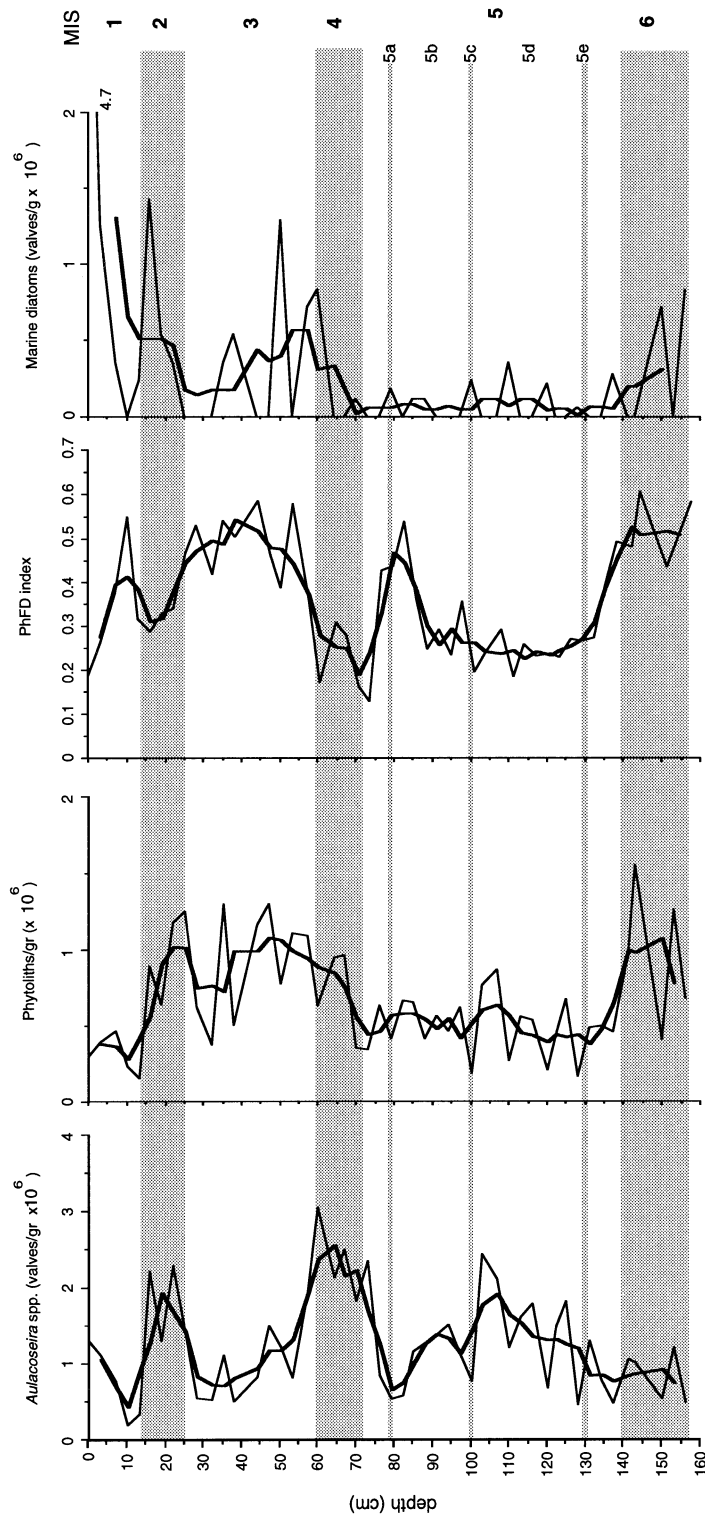


Fig. 6. Total abundance of various biosiliceous continental (freshwater diatom *Aulacoseira* sp. and phytoliths), PhFD index (Jansen and Van Iperen, 1991; see text for definition) and marine particles in core CAMEL-1. The thick lines are a three point moving average.

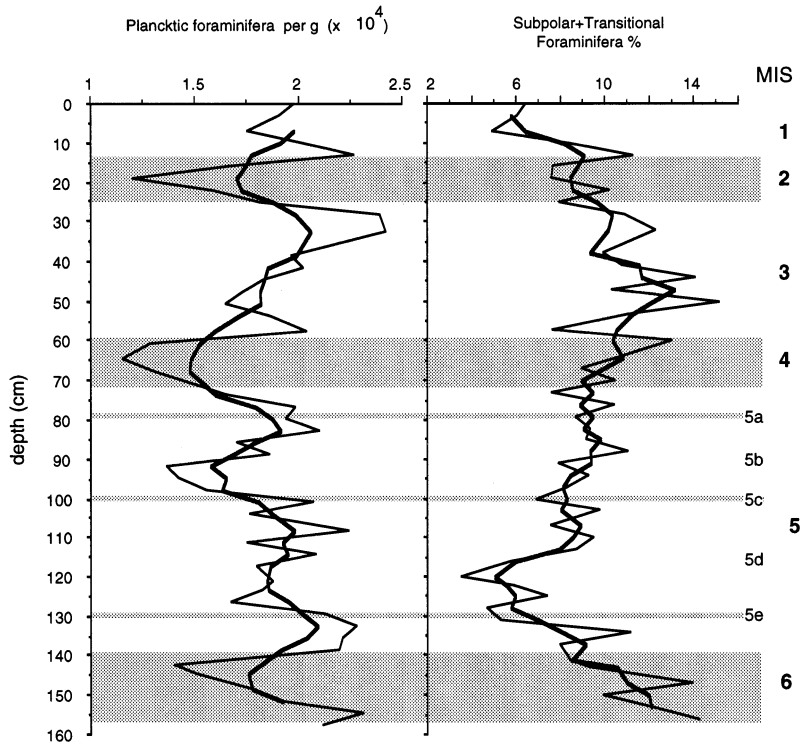


Fig. 7. Total abundance of planktic foraminifera and percentage of subtropical and transitional species in core CAMEL-1 (see Appendix). Thick lines are a three-point moving average.

boundary. *Helicosphaera* spp. show the lowest abundances here (Figs. 3–5). Phytoliths are very abundant in MIS 3, although well-defined minima are observed close to the MIS3/2 boundary. Fresh-water diatoms decrease from the MIS 4/3 boundary towards the top of MIS 3. The PhFD index shows high values, similar to those observed during the top of MIS 6. Marine diatoms show a peak during this interval, decreasing in abundance at the top (Fig. 6). Foraminiferal abundance in MIS 3 is relatively high, especially at the top of MIS 3. However, a maximum in the abundance of subpolar-transitional species is observed in the middle part of MIS 3 (Fig. 7).

5.5. MIS 2

The abundance of coccolithophores in MIS 2 is relatively low, but similar to that recorded for MIS 5. In MIS 2 a high proportion of Reticulofenestrids and a reduction in *Florisphaera profunda* can be

observed. Moderate peaks of *Calcidiscus leptoporus* and *Syracosphaera* spp. and a progressive increase in *Helicosphaera* spp. are also observed during this interval. Conversely, *Umbilicosphaera* spp. show a progressive reduction (Figs. 3–5). High values of phytoliths and fresh-water diatoms and relatively low values in the PhFD index are seen in MIS 2, coinciding with low proportions of foraminifera and a progressive reduction in the abundance of cold species (Figs. 6 and 7).

5.6. Holocene

The Holocene is characterized by a relative high abundance of Reticulofenestrids (mainly *Emiliania huxleyi*). *Helicosphaera* spp. increase dramatically and *Umbilicosphaera* spp. *Syracosphaera* spp. and *Calcidiscus leptoporus* decrease (Figs. 3–5). Phytoliths and *Aulacoseira granulata* show the lowest values, but the PhFD index show relatively high values (Fig. 6), and planktic foraminifers

occur in relatively high proportions, with a clear reduction in the abundance of subpolar and subtropical species (Fig. 7). The high marine diatom abundance observed in the upper part of the core is interpreted as a preservational effect (Fig. 6).

6. Discussion

The Coccolithophore assemblages observed in the Sierra Leone Rise region for the last 140 kyr are characteristic of a tropical mesotrophic/oligotrophic environment, with a relatively low nutricline (Winter et al., 1994; Jordan and Chamberlain, 1997). This situation is consistent with a high or relatively high proportion of *Florisphaera profunda*, an inhabitant of the current tropical LPZ in tropical and subtropical environments (Okada and Honjo, 1973). The low abundance of marine diatoms is also consistent with this scenario. Although these conditions prevailed over the last 140 kyr, quantitative changes in the coccolithophore assemblages allow us to recognize paleoecologically significant changes that reflect different paleoceanographic conditions.

Two main factors can be invoked to explain the distribution of the coccolithophore assemblages, namely: variations in surface water temperature and the nutrient content distribution in the water column. These factors are sometimes difficult to separate in tropical regions. Studying planktic foraminifera in different sites in the tropical equatorial east Atlantic, Mix and Morey (1996) and Jansen et al. (1996), interpreted alternative upwelling and advection from the Benguela Current during glacial periods, linked to an intensification of the trade winds (especially during the 'ice growth' phase). Both upwelling and advection pulses along the latest Pleistocene show a 23 kyr pattern. Molino and McIntyre (1990, 1991) demonstrated that nutricline (and thermocline) dynamics and surface water productivity were affected by precessional-forced changes in trade-wind intensity and subsequent fluctuations in equatorial Atlantic divergence. Beaufort et al. (1997) observed a clear negative relationship between primary productivity and *Florisphaera profunda* abundance in the Indian Ocean. These parameters

have been linked to insolation, which is a dominant precessional component instead of the dominant periodicities of ice sheet dynamics (Shackleton and Opdike, 1973; Imbrie et al., 1984).

In core CAMEL-1, the maxima in the *N* ratio are interpreted as relative increases in productivity as a consequence of a rise in the nutricline. In order to test the possible influence of the precessional component, we filtered the *N* ratio data and carried out spectral analyses using the program of Paillard et al. (1996) (Figs. 8 and 9). Peaks in this ratio occur in MIS 6, 5d, 5b, and 4, the top of 3 and 2. Between 140 and 80 kyr, these high productivity episodes correlate with low Northern Hemisphere summer (or high winter) insolation values (Perihelion during in the boreal summer). From MIS 4 to the Holocene, maxima in productivity occurred slightly before maxima in the boreal summer insolation (Fig. 8). The maximum abundance in *Gephyrocapsa oceanica* confirms the increase in high productivity in MIS 6. This species is widely reported as a warm water species with a preference for marginal seas (McIntyre and Bé, 1967; Okada and Honjo, 1973; Jordan et al. 1996). Winter (1982) and Winter and Martin (1990) reported a link between *G. oceanica* and high fertility and neritic environments, and concluded that peaks of this species are related to high productivity pulses. This is consistent with the studies of Ziveri et al. (1995) in the Gulf of California. In the Benguela area, Giraudeau (1992) observed that this species is linked to relatively warm and high nutrient-content surface waters; its presence in cold and fertile waters is scarce. Prell et al. (1980) linked this species to Agulhas Current tropical waters. Our *G. oceanica* are correlated with the *Gephyrocapsa* Larger group of Bollmann (1997), characteristic of coastal upwelling regions (Fig. 5). However, in core CAMEL-1, their abundance during other high production episodes is not significant.

Although the number of marine diatom valves is scarce, we observed maxima of these organisms in MIS 6, the top of 4, the base of 3 and 2, and these are interpreted as reflecting high productivity. The presence of *Thalassionema nitzchioides*, an upwelling-related taxon (Bárcena and Abrantes, 1998), agrees with this idea. As commented above,

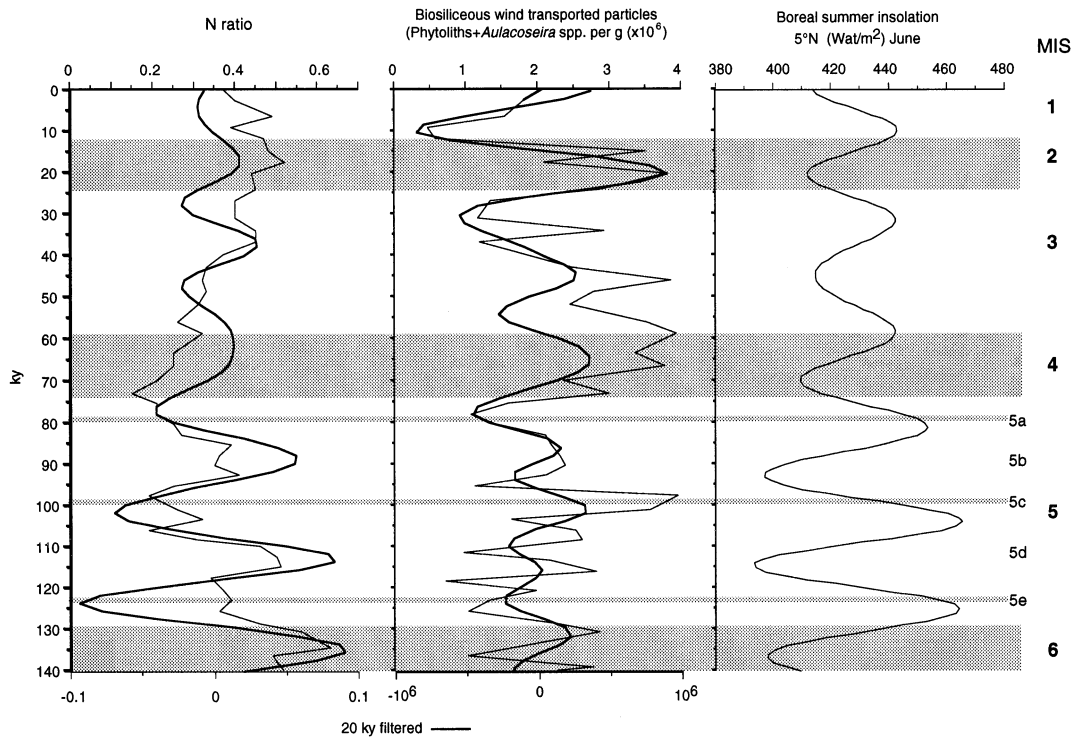


Fig. 8. N ratio ($N = R/R + F$; R = Reticulofenestrads; F = *Florisphaera profunda*; see text for definition), wind transported particles and Boreal summer insolation for the last 140 kyr in core CAMEL-1. For the 20 kyr filtered data the Paillard et al. (1996) program was used. Astronomical data from Laskar (1990).

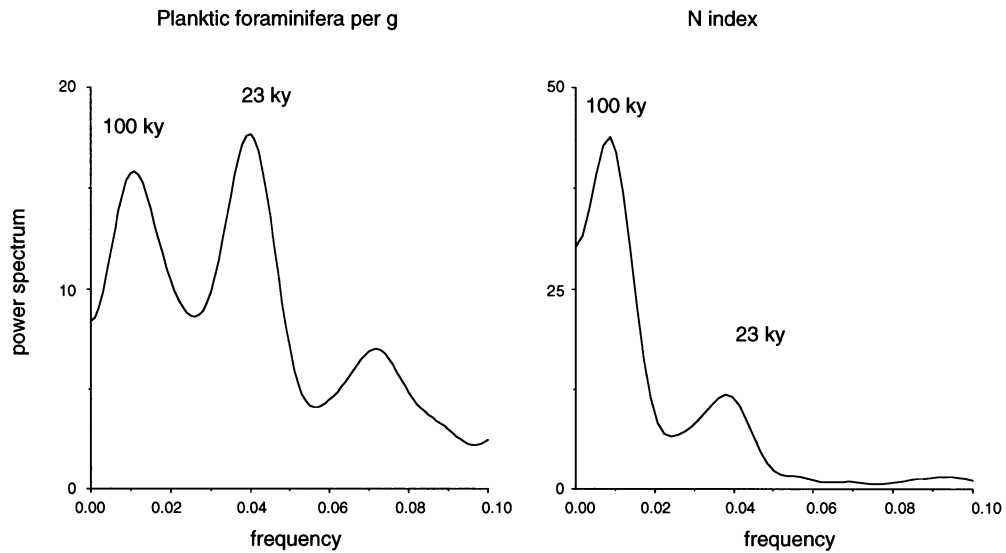


Fig. 9. Spectral analysis of planktic foraminifera per gram, and N ratio ($N = R/R + F$; R = Reticulofenestrads; F = *Florisphaera profunda*; see text for definition) in core CAMEL-1. Time series of 140 kyr interpolated at 2 kyr intervals. Bandwidth $0.020807 \text{ kyr}^{-1}$.

the Holocene marine-diatom peak is interpreted as preservational. A comparable pattern can be observed in the subpolar/transitional planktic foraminifera, with a maximum of these cold high-productivity species in MIS 6. From the top of MIS 4 to the Holocene, high proportions of these species are recorded, especially in the lower and middle part of MIS 3.

Taking into account all the micropaleontological groups studied, we infer high productivity intervals in MIS 6, 5d, 5b, 4, 3 and 2. This model is similar to that proposed by Jansen and Van Iperen (1991) in the Zaire Fan. For these intervals, Jansen et al. (1996) interpreted an intensification in the equatorial Atlantic upwelling.

Variations in primary production have a clear precessional component, which is also observed here. However, the continuous and abundant presence of *Florisphaera profunda* as the dominant coccolithophore species and the low abundance of marine diatoms are in agreement with the persistence of oligotrophic conditions over the last 140 kyr interval studied.

McIntyre et al. (1989) concluded that equatorial divergence is at a minimum when the perihelion is centred on the boreal summer because the North African monsoon is strong and the zonal component of the tropical easterlies is weak. This scenario is supported by our data from core CAMEL-1 pointing to the high abundance of organic wind-transported particles. In these groups we included fresh-water diatoms, originally produced in lakes and wind-transported after drying, and phytoliths, siliceous particles within terrestrial grasses injected into the atmosphere during dry-season brush fires (Pokras and Mix, 1985, Stabell, 1986, Pokras, 1987, Romero et al., 1999). We observed maxima of these organic transported particles in MIS 6, 5c, 4, middle part of 3, and 2, which are intervals of boreal summer insolation minima (Fig. 8). We conclude that during these intervals the NE trades were the dominant component. Since planktic foraminifera and the terrigenous component are the two main constituents of the sediment, we conclude that planktic foraminifera contents were mainly controlled by fluctuations in terrigenous eolic accumulation rates. The higher terrigenous input during glacials reduced the concentration of plank-

tic foraminifera in the sediment. Therefore, planktic foraminifera per can be considered a good proxy to estimate terrigenous wind input into the region. Spectral analysis revealed a high variance concentrations at 100 and especially at 23 kyr periods, suggesting a strong precessional component in the record of terrigenous input from the continent (Fig. 9). As previously posited by Molino and McIntyre (1990) this situation is consistent with an intensification in equatorial divergence that affected the core CAMEL-1 area. Schneider et al. (1996) have reported the same pattern of paleoproductivity in the east Equatorial Atlantic [trade wind-forced 23 kyr-cycles and advection of the Benguela Current (BC) waters to the north]. Abrantes (1991) has reported increasing upwelling rates in the Equatorial divergence and W African continental margin for glacial intervals. Hooghiemstra (1989) also inferred the existence of high wind strengths in MIS 6 and 2. A relationship appears between organic wind-transported particles and the N ratio for MIS 6, 5e, 5a, 2 and the Holocene; this is interpreted as an intensification of divergence due to wind strength, which produces a rise in the nutricline in the area. An exception occurs in 5c and partially in MIS 3, where the opposite trend between both indices is seen. Here, this is interpreted as high productivity pulses under a regime of relatively weak atmospheric circulation. As we mentioned before, same pattern was observed in the Gulf of Guinea by Dupont et al. (1998) during MIS 3, and was interpreted as a nutrient input from the BC. In the same area, Mix and Morey (1996) inferred an increase in the trade winds and equator upwelling during ice growth and glacial intervals, with a clear influence (advection) from the BC. Northern displacements of oceanographic features in the Gulf of Guinea region, such as the Angola–Benguela Front, have been correlated with minimum SST temperatures in the Pacific and Arabian Sea (Jansen et al., 1996). In both cases, two clear eccentricity (100 kyr) and precession (23 kyr) components are observed. The same pattern can be observed in the CAMEL-1 total of planktic foraminifera (g^{-1}) and N ratio records (Fig. 9). These episodes of advection in the Southern Tropical Atlantic are coupled with an intensification in the

NEC, Guinea Current (GC) and Canary Current (CC).

Wind dynamics also affects other systems. The increase in subpolar-transitional planktic foraminifera species (Kipp, 1976; Ruddiman and McIntyre, 1976 — see the Appendix) in MIS 6, and from 4 to 2 can also be interpreted here as a response to the enhancement in the NEC, as well as in the GC and CC. This situation is consistent with the ITCZ located at latitudes south of the region studied (Fig. 1). During interglacial periods, a reduction in the NEC occurs paralleling a reduction in intensity in atmospheric circulation patterns.

This interpretation is partially confirmed by the maxima of the relatively cold coccolithophorids in cold MIS 6, 5d, 5b, 4, and especially 3. *Gephyrocapsa muelleriae* (the most abundant taxon from the 'medium *Gephyrocapsa*' — Fig. 5) is generally considered to be a cold Atlantic species (Jordan et al., 1996; Flores et al., 1997). Additionally, the medium-sized species *Gephyrocapsa caribbeanica* in the North Atlantic is also interpreted as a cold species, although it is especially abundant below MIS 7 (Weaver and Thomson, 1993; Flores, in Villanueva, 1996). Wells and Okada (1996) linked this species with *Coccolithus pelagicus*, suggesting a relationship with cold conditions. Bollmann (1997) includes *G. muelleriae* in the *Gephyrocapsa* Cold group and *G. caribbeanica* in the *Gephyrocapsa* Oligotrophic group. We include *G. muelleriae* and *G. caribbeanica* in the medium-sized *Gephyrocapsa* complex (between 3 and 5 μm). Although *G. muelleriae* is the dominant species, integrated *G. muelleriae*/*G. caribbeanica* forms are frequent. Low abundances of medium and small *Gephyrocapsa* are observed in MIS2, coinciding with a clear increase in *Emiliana huxleyi*, an evolution-related event (Fig. 5). The recording of other coccolithophore species that are more abundant in subtropical or tropical waters, such as *Syracosphaera* spp. (Weaver, 1983; Jordan et al., 1996), *Umbilicosphaera sibogae* (McIntyre and Bé, 1967; Okada and McIntyre, 1979) or *Calcidiscus leptoporus* (Wells and Okada, 1996) in core CAMEL-1, is not well understood. Factors other than temperature and paleoproductivity must be invoked to explain their distribution.

The different types of behavior of the two types of organic wind-transported particles is also interesting. The abundance of the fresh-water diatom *Aulacoseira granulata* is a good proxy for arid conditions on the continent in this region. Valves of this organism can be transported after lakes depletion (Parmenter and Folger, 1974; Melia, 1984; Pokras and Mix, 1985; Stabell, 1986; Pokras, 1987; Abrantes, 1991, Romero et al., 1999). In the CAMEL-1 position, distant from the continent, without important river systems close and in an oceanic rise, wind is the main factor of transport of continental organic particles. Consequently, low values in the PhFD index are interpreted here as indicators of relatively arid conditions. This pattern is opposite to that reported for the Zaire Fan by Jansen and Van Iperen (1991), because in this region diatoms come from a river environment, and peaks in these organisms represent humid conditions. According to our PhFD index interpretation, MIS 5e, 5d, 5c, 4 and 2 (coinciding with peaks of *A. granulata*) represent arid conditions in the northwest African region; conversely, the top of MIS 6, 5a and 3 (with peaks in phytoliths) are interpreted as relatively humid intervals, with a more intense seasonality. These data have been partially confirmed by Pokras (1987), who interpreted aridification in MIS 5, and Abrantes (1991), who observed an increase in aridification, especially in 5d and between 5c/5b. Conversely, Causse et al. (1989) described an increase in precipitation in North Africa in MIS 5 (especially ca. MIS 5e.), coinciding with heavy monsoons (Prell and Campo, 1986). Jansen and Van Iperen (1991) interpreted dry conditions on the African continent in MIS 6, 5e, 5a to the top of 3 and 2. According to our data, a relative aridification occurred during MIS 5, with wet pulses ca. MIS 5e, 5c and 5a (Fig. 6). In MIS 4 and 2, the strong NE wind coincided with the driest conditions on the African continent (Sarnthein et al., 1982). Based on quartz and pollen features, Thiede et al. (1982) and Rognon (1987) interpreted arid conditions in North Africa during the LGM. The same pattern is observed in core CAMEL-1.

In our core, the peaks in phytoliths observed in MIS 6, 5c, and 4 to 2 are interpreted as corresponding to dry episodes with marked seasonality and a

Appendix

Coccolithophores	No. of coccoliths per coccosphere (Knappertsbusch, 1993; Kleijne, 1993)
<i>Calcidiscus leptoporus</i> (Murray and Blackman, 1898) Loeblich and Tappan (1978)	31
<i>Discosphaera tubifera</i> (Murray and Blackman, 1898) Ostenfeld, 1900	64
<i>Emiliania huxleyi</i> (Lohmann, 1902) Hay and Mohler in Hay et al. (1967)	23
<i>Florisphaera profunda</i> Okada and Honjo (1973)	76
Small <i>Gephyrocapsa</i> (<3 µm)	
<i>Gephyrocapsa aperta</i> Kamptner (1963)	19
<i>Gephyrocapsa ericsonii</i> McIntyre and Bé (1967)	19
Medium <i>Gephyrocapsa</i> (3–5 µm)	
<i>Gephyrocapsa caribbeanica</i> Boudreaux and Hay (1967)	19
<i>Gephyrocapsa muelleriae</i> Bréhéret (1978)	19
<i>Gephyrocapsa oceanica</i> Kamptner (1943)	19
<i>Helicosphaera carteri</i> (Wallich, 1877) Kamptner (1954)	24
<i>Neosphaera coccolithomorpha</i> (Lecal-Schlauder, 1950)	30
<i>Rhabdosphaera clavigera</i> (Murray and Blackman, 1898)	20
<i>Syracosphaera pulchra</i> (Lohmann, 1902)	52
<i>Umbellosphaera tenuis</i> (Kamptner, 1937) Paasche (1955)	19
<i>Umbilicosphaera sibogae</i> (Weber-van Bosse, 1901) Gaarder (1970)	204
<hr/>	
Planktic foraminifera	
<hr/>	
Subpolar and/or transitional species (Ruddiman and McInyre, 1976)	
<i>Globigerina bulloides</i> (d'Orbigny, 1826)	
<i>Globorotalia inflata</i> (d'Orbigny, 1839)	
<i>Neogloboquadrina pachyderma</i> (Ehrenberg, 1861)	
<i>Neogloboquadrina dutertrei</i> (d'Orbigny, 1893)	
<i>Turborotalita quinqueloba</i> (Natland, 1938)	
Tropical/subtropical species (Ruddiman and McInyre, 1976)	
<i>Globigerinoides sacculifer</i> (Brady, 1877)	
<i>Globigerinoides ruber</i> (d'Orbigny, 1839)	
<i>Pulleniatina obliquiloculata</i> (Parker and Jones, 1865)	
<hr/>	
Diatoms	
<hr/>	
Marine	
<i>Azpeitia nodulifera</i> (Schmidt) (Fryxell and Sims, 1986)	
<i>Alveus marinus</i> (Grunow) (Kaczmarska and Fryxell, 1996)	
<i>Coscinodiscus marginatus</i> (Ehrenberg, 1841)	
<i>Thalassionema nitzschioides</i> (Grunow) (Grunow, 1881)	
Freshwater	
<i>Aulacoseira granulata</i> (Ehrenberg) (Thwaites, 1848)	
<i>Cyclotella meneghiniana</i> (Kützing, 1844)	
<i>Cyclotella ocellata</i> (Pantocsek, 1902)	

probable intensification of brush-fires: large amounts of particles from tall-grass savannah produced during the humid season are injected into the atmosphere during dry-season brush fires and transported through the atmosphere to the marine realm (Pokras and Mix, 1985). In the Sierra Leone ODP Site 668, Bird and Cali (1998) interpreted intense burning on the African continent in MIS 6, 4 and 2; during these intervals, the percentage of aeolian particles also rose. Schneider et al. (1996) interpreted humid conditions in Equatorial Africa in MIS 5e, 5c, the base of 3, the 3/2 transition and the Holocene.

7. Conclusions

- Wind intensity and direction control surface water dynamics in the oligotrophic tropical Atlantic. The oligotrophic environmental situation was dominant in the region during the last 140 kyr. However, small differences in the nutricline/thermocline position are interpreted as being linked to atmospheric pattern variations.
- The abundance of fresh-water diatoms in the Sierra Leone Rise is linked to aeolian intensity rather than to river input, and used here as a relative wind intensity proxy.
- In MIS 5d, 5b, 4 and 2, intensification in equatorial Atlantic divergence led to a shallow nutricline. At the same time, an increase in NE Trade wind intensity occurred, corresponding to arid conditions on the African continent. In MIS 6 and 3, wind strength intensity and dry environmental conditions were also dominant, but with a more intense seasonality in North Africa and a more intense NEC influence in the ocean. In MIS 5e, 5c and 5a, and, partly in MIS 3, a deeper nutricline was the dominant feature in the region.
- The precessional-forcing component is characteristic, but an eccentricity pattern linked to northern ice-sheet dynamics, both in coccolithophores and planktic foraminifera assemblages (total per gram and Subpolar-transitional ratio), is also observed. A similar and time-coupled pattern is observed in the South

Tropical Atlantic, but this can mainly be explained by advection from the Benguela Current.

- A humid African scenario in MIS 5e, 5c, 3 (partially) and the Holocene is consistent with weak NE trade winds and a relatively deep nutricline in the Sierra Leone Rise area.

Acknowledgements

Dr. Hisatake Okada, Dr. J.H.F. Jansen, Dr. Gabriel M. Filippelli, Dr. Jeremy Young and an anonymous referee are acknowledged for their valuable reviews and suggestions. The authors thank N. Skinner for revising the English version of the manuscript. Jesús Roncero is also acknowledged for his help in sample processing. Research Grants Nos. CICYT CLI962261-E and CLI98-1002-CO2 supported this study.

References

- Abelmann, A., Bock, U., Gersonde, R., Treppke, U.F., 2000. A revised preparation technique for siliceous microfossils. *Micropaleontology* (in press).
- Abrantes, F., 1991. Variability of upwelling off NW Africa during the latest Quaternary: diatom evidence. *Paleoceanography* 6 (4), 431–460.
- Bárcena, M.A., Abrantes, F., 1998. Evidence of a high productivity area off the coast of Malaga from studies on surface sediments. *Mar. Micropaleontol.* 35, 91–103.
- Bé, A.W.H., Damuth, J.E., Lott, L., Free, R., 1976. Late Quaternary climatic record in Western Equatorial Atlantic sediment. In: Cline, R.M., Hays, J.D. (Eds.), *Investigation of Late Quaternary Paleoclimatology and Paleoclimatology*, Geol. Soc. Am. Mem. 145, 165–200.
- Beaufort, L., Lancelot, Y., Chamberlin, P., Cayre, O., Vincent, E., Bassinot, F., Labeyrie, L., 1997. Insolation cycles as a major control of equatorial Indian Ocean primary production. *Science* 278, 1451–1454.
- Bird, M.I., Cali, J.A., 1998. A million-year record of fire in sub-Saharan Africa. *Nature* 394, 767–769.
- Bollmann, J., 1997. Morphology and biogeography of *Gephyrocapsa* coccoliths in Holocene sediments. *Mar. Micropaleontol.* 29, 319–350.
- Broecker, W.S., 1982. Glacial to interglacial changes in ocean chemistry. *Prog. Oceanog.* 11, 151–197.
- Causse, C.R., Casque, J.C., Fontes, F., Gasse, E., Gilbert, H., Ouezddou, B., Zouari, K., 1989. Two high levels of conti-

- mental waters in southern Tunisia chotts at 100 and 150 ka. *Geology* 17, 922–925.
- Dupont, L.M., 1999. Pollen and spores in marine sediments from the East Atlantic — a view from the ocean into de African continent. In: Fischer, G., Wefer, G. (Eds.), *Use of Proxies in Paleoceanography: Examples from the South Atlantic*. Springer-Verlag, Berlin, pp. 523–546.
- Dupont, L.M., Agwu, C.O.C., 1992. latitudinal shifts of forest and savanna in NW Africa during the Bruhnes chron: further marine palynological results from site M 16145 (9°N 19°W). *Veget. Hist. Archaeobot.* 1, 163–175.
- Dupont, L.M., Hooghiemstra, H., 1989. The Saharan–Sahelian boundary during the Bruhnes chron. *Act. Bot. Neerl.* 38, 405–415.
- Dupont, L.M., Weinelt, M., 1996. Vegetation history of the savanna corridor between the Guinean and the congolian rain forest during the last 150,000 years. *Veget. Hist. Archaeobot.* 5, 273–292.
- Dupont, L.M., Marret, F., Winn, K., 1998. Land-sea correlation by means of terrestrial and marine palynomorphs from the equatorial East Atlantic: phasing of SE trade winds and the oceanic productivity. *Plaeogeogr., Palaeoclimatol., Palaeoecol.* 142, 51–84.
- Dupont, L.M., Schneider, R., Schmäser, A., Jahns, S., 1999. Marine-terrestrial interaction of climate changes in Western Equatorial Africa of the last 190,000 years. *Pal. Mr.* 26, 61–84.
- Ericson, D.B., Wollin, J., 1968. Pleistocene climates and chronology in deep-sea sediments. *Science* 162, 1227–1234.
- Eriksen, C.C., Katz, E.J., 1987. Equatorial dynamics. *Rev. Geophys.* 25, 217–226.
- Flores, J.A., Sierro, F.J., 1997. Revised technique for calculation of calcareous nannofossil accumulation rates. *Micro-paleontology* 43, 321–324.
- Flores, J.A., Sierro, F.J., Francés, G., Vázquez, A., Zamarreño, Y., 1997. The last 100,000 years in the western Mediterranean sea surface water and frontal dynamics as revealed by coccolithophores. *Mar. Micropaleontol.* 29, 351–366.
- Gardner, J.V., Hays, J.D., 1976. Responses of sea-surface temperatures and circulation to global climate change during the past 200,000 years in the eastern Equatorial Atlantic Ocean. *Geol. Soc. Am. Mem.* 145, 221–246.
- Garzoli, S.L., Katz, E.J., 1983. The forced annual reversal of the Atlantic North Equatorial Countercurrent. *J. Phys. Oceanogr.* 13, 2082–2090.
- Gasse, F., Stabel, B., Fourtanier, E., van Iperen, Y., 1989. *Quat. Res.* 32, 229–243.
- Giraudeau, J., 1992. Distribution of Recent nannofossils beneath the Benguela system: southwest African continental margin. *Mar. Geol.* 108, 219–237.
- Höflich, O., 1984. Climate of the South Atlantic Ocean. In: Van Loon, H. (Ed.), *World Survey of Climatology* vol. 15, *Climates of the Oceans*. Elsevier, Amsterdam, pp. 1–191.
- Hooghiemstra, H., 1989. Variations of the NW African trade wind regime during the last 140,000 years: changes in pollen flux evidence by marine sediments records. In: Leinen, M., Sarnthein, M. (Eds.), *Paleoclimatology and Paleometeorology: Modern and Past Patterns of Global Atmospheric Transport*. Kluwer, Dordrecht, pp. 733–770.
- Houghton, R.W., 1991. The relationship of sea surface temperature to thermocline depth at annual and interannual time scales in the tropical Atlantic Ocean. *J. Geophys. Res.* 96, 15173–15185.
- Imbrie, J., Hays, J.D., Martinson, D.G., McIntyre, A., Mix, A.C., Morley, J.J., Pisias, N.G., Prell, W.L., Shackleton, N.J., 1984. The orbital theory of Pleistocene climate: Support from a revised chronology of the marine $\delta^{18}\text{O}$ record. In: Berger, A.L., Imbrie, J., Hays, J., Kukla, G., Saltzman, B. (Eds.), *Milankovitch and Climate, Part 1*. Reidel, The Netherlands, pp. 269–305.
- Jansen, J.H.F., Van Iperen, J.M., 1991. A 220,000-year climatic record for the East Equatorial Atlantic Ocean and Equatorial Africa: evidence from diatoms and opal phytoliths in the Zaire (Congo) deep-sea fan. *Paleoceanography* 6, 573–591.
- Jansen, J.H.F., Alderliesten, C., Houston, C.M., De Jong, A.F.M., Van del Borg, K., Van Iperen, J.M., 1989. Aridity in equatorial Africa during the last 225,000 years: a record of opal phytoliths/freshwater diatoms from the Zaire (Congo) deep-sea fan (northeast Angola basin). *Radiocarbon* 31, 557–569.
- Jansen, J.H.F., Ufkes, E., Schneider, R.R., 1996. Late Quaternary movements of the Angola-Benguela Front SE Atlantic and implications for advection in the Equatorial Ocean. In: Wefer, G., Berger, W.H., Siedler, G., Webb, D.J. (Eds.), *The South Atlantic: Present and Past Circulation*. Springer-Verlag, Berlin, pp. 553–575.
- Jordan, R.W., Chamberlain, A.H.L., 1997. Biodiversity among Haptophyte algae. *Biodiversity and Conservation* 6, 131–152.
- Jordan, R.W., Zhao, M., Eglinton, G., Weaver, P.P.E., 1996. Coccolith and alkenone stratigraphy and palaeoceanography at an upwelling site off NW Africa ODP 658C during the last 130,000 years. In: Whatley, R., Mogueilevsky, A. (Eds.), *Microfossils and Oceanic Environments*, University of Wales, Aberystwyth Press. pp. 111–152.
- Kalu, A.E., 1979. The African dust plume: its characteristics and propagation across West Africa in winter. In: Morales, C. (Ed.), *Saharan Dust: Mobilization, Transport, Deposition*. Wiley, New York, pp. 95–118.
- Katz, E.J., Molinari, R.L., Cartwright, D.E., Hisard, P., Lass, H.U., deMesquita, A., 1981. The seasonal transport of Equatorial Undercurrent in the western Atlantic (during the Global Weather Experiment). *Oceanol. Acta* 4, 445–450.
- Kipp, N.G., 1976. New Transfer Function for Estimating Past Sea-Surface Conditions from Sea-Bed Distribution of Planktonic Foraminiferal Assemblages in the North Atlantic. In: Cline, R.M., Hays, J.D. (Eds.), *Investigation of Late Quaternary Paleoclimatology and Paleoclimatology*, *Geol. Soc. Am. Mem.* 145, 111–146.
- Kleijne, A., 1993. Morphology, taxonomy and distribution of extant Coccolithophorids (Calcareous nannoplankton), Ph.D. Thesis, University of Amsterdam.
- Knappertsbusch, M., 1993. Geographic distribution of living

- and Holocene coccolithophores in the Mediterranean Sea. *Mar. Micropaleontol.* 21, 219–247.
- Lange, C.B., Treppke, U.F., Fischer, G., 1994. Seasonal diatom fluxes in the Guinea basin and their relationships to trade winds, hydrography and upwelling events. *Deep-Sea Res.* 41, 859–878.
- Laskar, J., 1990. The chaotic motion of the solar system: a numerical estimate of the chaotic zones. *Icarus* 88, 266–291.
- Martinson, D.G., Pisias, N.G., Hays, J.D., Imbrie, J., Moore, T.C., Shackleton, N.J., 1987. Age dating and the orbital theory of the ice ages: development of a high-resolution 0 to 300,000-year chronostratigraphy. *Quat. Res.* 27, 1–29.
- McIntyre, A., Bè, A.W.H., 1967. Modern Coccolithophoridae of the Atlantic Ocean, placoliths and cyrtoliths. *Deep-Sea Res.* 14, 561–597.
- McIntyre, A., Ruddiman, W.F., Karlin, K., Mix, A.C., 1989. Surface water response of the equatorial Atlantic Ocean to orbital forcing. *Paleoceanography* 4, 19–55.
- Melia, M.B., 1984. The distribution and relationship between palynomorphs in aerosols and deep-sea sediments off the coast of Northwest Africa. *Mar. Geol.* 58, 345–371.
- Mix, A.C., Morey, A.E., 1996. Climate feedback and Pleistocene variations in the Atlantic South Equatorial Current. In: Wefer, G., Berger, W.H., Siedler, G., Webb, D.J. (Eds.), *The South Atlantic: Present and Past Circulation*. Springer-Verlag, Berlin, pp. 503–525.
- Molfino, B., McIntyre, A., 1990. Precessional forcing of nutricline dynamics in the equatorial Atlantic. *Science* 249, 766–769.
- Molfino, B., McIntyre, A., 1991. Nutricline variations in the equatorial Atlantic coincident with the Younger Dryas. *Paleoceanography* 5, 997–1008.
- Ning, S., Dupont, L.M., 1997. Vegetation and climate history of southwest Africa: a marine palynological record of the last 300,000 years. *Veget. Hist. Archeobot.* 6, 117–131.
- Okada, H., Honjo, S., 1973. The distribution of oceanic coccolithophorids in the Pacific. *Deep-Sea Res.* 20, 355–374.
- Okada, H., McIntyre, A., 1979. Seasonal distribution of modern Coccolithophores in the Western North Atlantic ocean. *Mar. Biol.* 54, 319–328.
- Okada, H., Well, P., 1997. Late Quaternary nannofossil indicators of climate change in two deep-sea cores associated with the Leeuwin Current off Western Australia. *Plaeoogeogr., Palaeoclimatol., Palaeoecol.* 131, 413–432.
- Paillard, D., Labeyrie, L., Yiou, P., 1996. Macintosh program performs time-series analysis. *Eos Trans. AGU* 77, 379
- Parmenter, C., Folger, D.W., 1974. Eolian biogenic detritus in deep-sea sediments: a possible index of equatorial Ice Age aridity. *Science* 185, 695–698.
- Peterson, R.G., Stramma, L., 1991. Upper-level circulation in the South Atlantic. *Progr. Oceanogr.* 26, 1–73.
- Pokras, E.M., 1987. Diatom record of late Quaternary climatic change in the eastern equatorial Atlantic and tropical Africa. *Paleoceanography* 2, 273–286.
- Pokras, E.M., Mix, A.C., 1985. Eolian evidence for spatial variability of late Quaternary climates in tropical Africa. *Quat. Res.* 24, 137–149.
- Pokras, E.M., Mix, A.C., 1987. Earth's precession cycle and Quaternary climatic change in tropical Africa. *Nature* 326, 486–487.
- Prell, W.L., Campo, E.V., 1986. Coherent response of Arabian Sea upwelling and pollen transport to late Quaternary monsoonal winds. *Nature* 323, 526–528.
- Prell, W.L., Hutson, W.H., Williams, D.F., 1980. Surface circulation of the Indian Ocean during the Last Glacial Maximum, approximately 18,000 yr B.P. *Quat. Res.* 14, 309–336.
- Prospero, J.M., Carlson, T.N., 1972. Vertical and aerial distribution of Saharan dust over the western equatorial North Atlantic Ocean. *J. Geophys. Res.* 77, 5255–5265.
- Richardson, P.L., Walsh, D., 1986. Mapping climatological seasonal variations of surface currents in the tropical Atlantic using ship drifts. *J. Geophys. Res.* 91 (537), 10537–10550.
- Rognon, P., 1987. Late Quaternary climatic reconstruction for the Maghreb (North Africa). *Palaeogeogr., Palaeoclimatol., Palaeoecol.* 58, 11–34.
- Romero, O.E., Lange, C.B., Swap, R., Wefer, G., 1999. Eolian-transported freshwater diatoms and phytoliths across the equatorial Atlantic record: temporal changes in Saharan dust transport patterns. *J. Geophys. Res.* 104, 3211–3222.
- Rosignol-Strick, M., 1983. African monsoons, an immediate climate response to orbital insolation. *Nature* 303, 46–49.
- Ruddiman, W.F., Janecek, T., 1989. Pliocene-Pleistocene biogenic and terrigenous fluxes at equatorial Atlantic sites 662, 663, and 664. *Proc. ODP, Sci. Results* 108, 211–240.
- Ruddiman, W.F., McIntyre, A., 1976. Northeast Atlantic paleoclimatic changes over the past 600,000 years. In: Cline, R.M., Hays, J.D. (Eds.), *Investigation of Late Quaternary Paleoclimatology and Paleoclimatology*, *Geol. Soc. Am. Mem.* 145, 111–146.
- Ruddiman, W.F., Sarnthein, M., Backman, J., Baldauf, J.G., Curry, W., Dupont, L.M., Janecek, T., Pokras, E.M., Raymo, M.E., Stabell, B., Stein, R., Tiedemann, R., 1989. Late Miocene to Pleistocene evolution of climate in Africa and the low-latitude Atlantic: overview of Leg 108 results. *Proc. ODP, Sci. Results* 108, 463–484.
- Sarnthein, M., Thiede, U., Pflaumann, H., Erlenkeuser, D., Fütterer, D., Koopmann, H., Lange, H., Seibold, E., 1982. Atmospheric and oceanic circulation patterns off northwest Africa during the last 25 million years. In: von Rad, U., Hinz, K., Sarnthein, M., Seibold, E. (Eds.), *Geology of the Northwest African Continental Margin*. Springer, New York, pp. 584–604.
- Schneider, R.R., Müller, P.J., Ruhland, G., Meinecke, H., Schmidt, H., Wefer, G., 1996. Late Quaternary surface temperatures and productivity in the East-Equatorial South Atlantic: response to changes in Trade/Monsoon wind forcing and surface water advection. In: Wefer, G., Berger, W.H., Siedler, G., Webb, D.J. (Eds.), *The South Atlantic: Present and Past Circulation*. Springer-Verlag, Berlin, pp. 527–551.
- Schrader, H.J., Gersonde, R., 1978. Diatoms and silicoflagellates. Micropaleontological counting methods and techniques an exercise on an eight metres section of the Lower

- Pliocene of Capo Rosello, Sicily. *Utrecht Bull. Micropaleontol.* 17, 129–176.
- Schütz, L., 1980. Long range transport of desert dust with emphasis on the Sahara. In: Kneip, T.J., Lioy, P.J. (Eds.), *Aerosols: Anthropogenic and Natural, Sources and Transport*, Ann. New York Acad. Sci. 338, 515–532.
- Shackleton, N.J., Opdike, N.D., 1973. Oxygen isotope and paleomagnetic stratigraphy of Equatorial Pacific core V28-238: Oxygen isotope temperature and ice volumes on a 10,000 year and 100,000 year time scale. *Quat. Res.* 3, 39–55.
- Stabell, B., 1986. Variations of diatom flux in the eastern equatorial Atlantic during the last 400,000 years (“Meteor” cores 13519 and 13521). *Mar. Geol.* 72, 305–323.
- Tetzlaff, G., Wolter, K., 1980. Meteorological patterns and the transport of mineral dust from the North African Continent. *Palaeoecol. Afr.* 12, 31–42.
- Thiede, J., Suess, E., Muller, P.J., 1982. Late Quaternary fluxes of major sediment components to the sea floor at the north-west African continental slope. In: von Rad, U., Hinz, K., Sarnthein, M., Seibold, E. (Eds.), *Geology of the Northwest African Continental Margin*. Springer, New York, pp. 605–631.
- Thierstein, H.R., Geitzenauer, K.R., Molfino, B., Shackleton, N.J., 1977. Global synchronicity of late Quaternary coccolith datum levels: validation by oxygen isotopes. *Geology* 5, 400–404.
- Tiedemann, R., Sarnthein, M., Stein, R., 1989. Climatic changes in the western Sahara: aeolo-marine sediment record of the last 8 million years (Sites 657–661). *Proc. ODP, Sci. Results* 108, 241–277.
- Treppke, U.F., Lange, C.B., Wefer, G., 1996. Vertical fluxes of diatoms and silicoflagellates in the eastern equatorial Atlantic, and their contribution to the sedimentary record. *Mar. Micropaleontol.* 28, 73–96.
- Verstraete, J.-M., 1992. The seasonal upwelling in the Gulf of Guinea. *Prog. Oceanogr.* 29, 1–60.
- Villanueva, J., 1996. Estudi de les variacions climàtiques y oceanogràfiques a l’Atlàntic Nord durant els últims 300.000 anys mitjançant l’anàlisi de marcadors moleculars, Ph.D. Universitat Ramon Llull. Barcelona.
- Voituriez, B., Herland, A., 1977. Étude de la production pélagique de la zone équatoriale de l’Atlantique a 4°W. *Cahier ORSTROM, sér. Océanogr.* 15, 313–331.
- Weaver, P.P.E., 1983. An integrated stratigraphy of the Upper Quaternary of the King’s Trough flank area EN Atlantic. *Oceanol. Acta* 6 (4), 451–456.
- Weaver, P.P.E., Thomson, J., 1993. Calculating erosion by deep-sea turbidity currents during initiation and flow. *Nature* 364, 136–138.
- Wells, P., Okada, H., 1996. Holocene and Pleistocene glacial paleoceanography off southeastern Australia, based on foraminifers and nannofossils in Vema cored hole V18-222. *Australian J. E. Sci.* 43, 509–523.
- Winter, A., 1982. Paleoenvironmental interpretation of Quaternary coccoliths assemblages from the Gulf of Aqaba (Elat), Red Sea. *Rev. Esp. Micropaleontol.* 14, 197–223.
- Winter, A., Martin, K., 1990. Late Quaternary history of the Agulhas Current. *Paleoceanography* 5 (4), 479–486.
- Winter, A., Jordan, R.W., Roth, P.H., 1994. Biogeography of living coccolithophores in ocean waters. In: Winter, A., Sieser, W.G. (Eds.), *Coccolithophores*. Cambridge University Press, Cambridge, pp. 161–177.
- Ziveri, P., Thunell, R.C., Rio, D., 1995. Export production of coccolithophores in an upwelling region: Results from San Pedro Basn, Southern California Borderlands. *Mar. Micropaleontol.* 24, 335–358.